

## Heterogeneous Exchange of Mixed Precipitates. [AgI + PbI<sub>2</sub>]<sub>solid</sub> in KI Solution

R. Despotović, Z. Despotović, S. Popović, L. Prodanović and B. Tomaš

Received September 26, 1975

Laboratory of Colloid Chemistry, »Ruđer Bošković« Institute, 41001 Zagreb, Croatia, Yugoslavia

The heterogeneous exchange process of mixed AgI + PbI<sub>2</sub> precipitates with iodide from the KI solution was studied using <sup>131</sup>I. The systems under examination were prepared *in statu nascendi* at 293 K. Radiometrically determined solubility, differential thermal analysis and X-ray diffraction analysis data were compared with radioanalytical results of the heterogeneous exchange processes. The results show strong mutual dependence of the metal halides present throughout the exchange process. The quantitative analysis of radiometric data indicates the specific influence of lead iodide onto silver iodide particles during the Ostwald's ripening process.

### INTRODUCTION

The process of heterogeneous exchange of precipitates is convenient for obtaining information on the equilibration of the precipitates or solids with the supernatant liquor or the surrounding solution<sup>1</sup>. Many results of heterogeneous exchange of constituent ions are obtained in the simple »solid (crystal precipitate)/liquid (electrolyte solution)« systems, but rarely for systems with mixed precipitates<sup>2</sup>. In order to determine the course of heterogeneous exchange in mixed systems the [AgI + PbI<sub>2</sub>]<sub>solid</sub> ↔ I<sup>-</sup><sub>electrolyte</sub> system was chosen and radioanalytical results are given in the present paper and compared with X-ray analysis, differential thermal analysis and literature data<sup>3-6</sup>.

### EXPERIMENTAL

#### Materials

All chemicals used were of p. a. grade. Using the chromate method the silver nitrate solution was standardized by a standard NaCl solution. The lead nitrate solution was standardized by the molybdenate method. The potassium iodide solution was standardized using di-iododimethylfluorescein as an end-point indicator. Solutions of potassium nitrate were prepared by weighing the p. a. chemical. Radioiodine <sup>131</sup>I was a solution of carrier free <sup>131</sup>I<sup>-</sup> of NaI form. The water used was doubly distilled in a Duran 50 apparatus.

#### Radioanalytical Experiments

(i) *Solubility Determination.* — All the systems described were prepared with an excess of iodide ions in the liquid phase using the *'in statu nascendi'* method and thermostatted at 293.0 ± 0.2 K. Solutions containing cationic components (Ag<sup>+</sup>, Ag<sup>+</sup> + Pb<sup>2+</sup>, Pb<sup>2+</sup>) were added into agitated KI solutions labelled by <sup>131</sup>I with or without added KNO<sub>3</sub> then stirred 5 minutes and left for  $t_A = 10000$  minutes. The clear supernatant was used for the determination of equilibrium radioactivity  $A_\infty$

by using an EKCO Electronics well-type NaI(Tl) scintillation counter and a semi-automatic scaler. The sample with initial radioactivity  $A_0$  was prepared in the same manner as above but with no precipitated metal halides in the systems. The total amount of iodide in the liquid phase is  $n_{\Sigma}^L$ , in the solid phase  $n_{\Sigma}^S$  and the ratio is  $\alpha_{\Sigma} = n_{\Sigma}^S/n_{\Sigma}^L$ . The solubility of metal iodide is presented as an average  $\alpha_{\Sigma}$  value of data obtained for seven systems prepared in the same way (Figure 1 and Table I.)

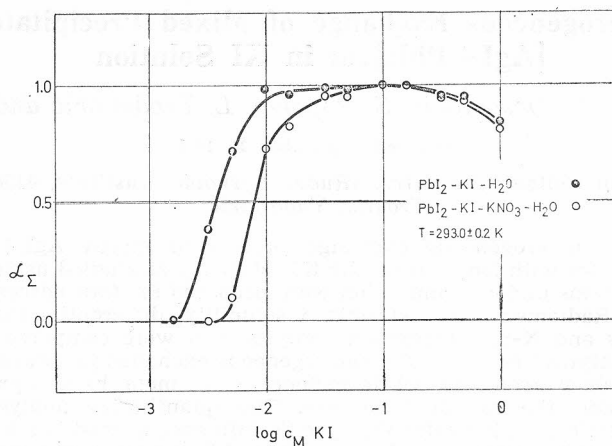


Figure 1. Ratio  $\alpha_{\Sigma}$  plotted against potassium iodide concentrations  $c_M$  (molarity, log scale) for the  $PbI_2 + KI$  systems obtained by direct mixing of  $Pb(NO_3)_2$  and  $KI$  solutions (full circles) and for the systems prepared by mixing of  $Pb(NO_3)_2$  solutions with  $KI + KNO_3$  solutions (open circles) at  $293.0 \pm 0.2$  K.

TABLE I

$\alpha_{\Sigma}$  Values for  $AgI + PbI_2 + KI + KNO_3$  Systems at Various Mole Fractions  $f$  of  $AgI$  ( $f_{AgI}$ ) and  $PbI_2$  ( $f_{PbI_2}$ ) in the Presence of 0.05 M  $KI$  and  $KNO_3$  at 293 K.

$f_{AgI}$	1.0	0.95	0.90	0.85	—
$f_{PbI_2}$	—	0.05	0.10	0.15	1.0
$\alpha_{\Sigma}$	$1.009 \pm 0.0014$	$0.997 \pm 0.003$	$1.001 \pm 0.003$	$1.013 \pm 0.001$	$1.002 \pm 0.004$

(ii) *Heterogeneous Exchange Experiments.* — Systems prepared in the same way as for solubility determination (except that the systems were labelled after  $t_A = 10$  and/or 10000 minutes), were used in examinations of the heterogeneous exchange processes. The initial and equilibrium radioactivities  $A_0$  and  $A_{\infty}$  were determined in the same way. After chosen time intervals ( $t_E = 30, 100, 300, 1500, 3000$  and 10000 minutes) the clear supernatant was taken off for measurements of the radioactivity  $A_t$ . The results were expressed (Figures 2—6) in terms of the fraction of exchange  $F = (A_0 - A_t)/(A_0 - A_{\infty})$  using average values obtained for three samples separately prepared under equal conditions.

(iii) *Differential Thermal Analysis.* — In order to obtain the phase diagram differential thermal analysis (DTA) was used. The apparatus was a commercial unit manufactured by Gebrüder Netzsch (Selb/Bayern, Germany). The measuring head for dynamical differential calorimetry according to H. E. Schwiete<sup>7</sup> with an

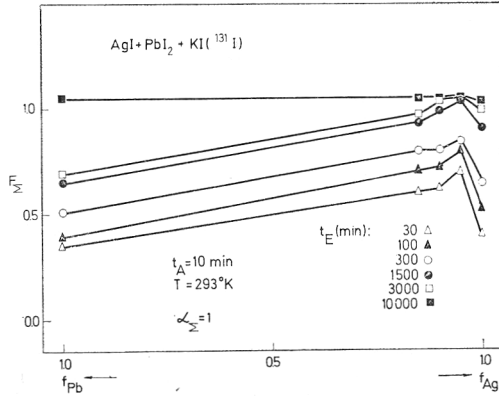
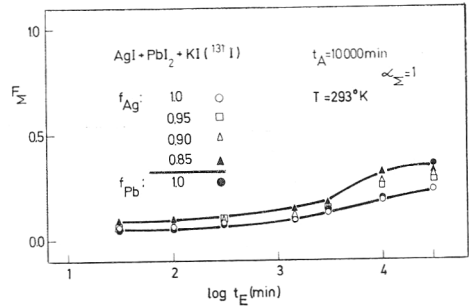
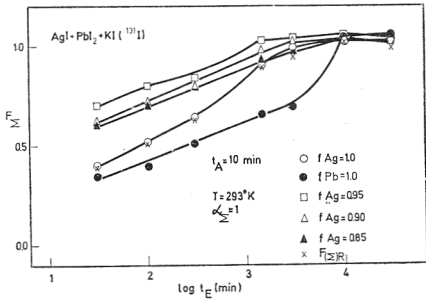


Figure 2. Exchange fraction,  $F_{\Sigma}$ , plotted against the mole fractions,  $f$ , of lead iodide ( $f_{Pb}$ ) and silver iodide ( $f_{Ag}$ ) in (i)  $PbI_2 + KI(^{131}I)$ ; (ii, iii, iv)  $PbI_2 + AgI + KI(^{131}I)$  and (v)  $AgI + KI(^{131}I)$  systems aged for  $t_A = 10$  minutes and at various exchange times  $t_E = 30, 100, 300, 1500, 3000$  and  $10000$  minutes at  $293$  K.



Figures 3 (left) and 4 (right). Exchange fraction,  $F_{\Sigma}$ , plotted against exchange time  $t_E$  (in minutes, logarithmic scale) in (i)  $AgI + KI(^{131}I)$ ; (ii)  $PbI_2 + KI(^{131}I)$  and (iii, iv, v)  $AgI + PbI_2 + KI(^{131}I)$  systems aged for  $t_A = 10$  minutes (Figure 3.)  $t_A = 10000$  minutes (Figure 4.) at  $293$  K in aqueous media. The computed  $F_{(\Sigma)R}$  [eq. 2] data are labelled by x.

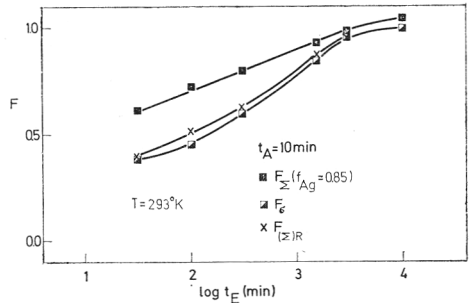
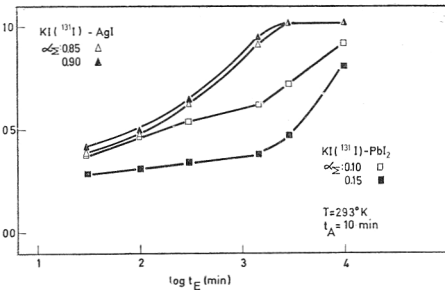


Figure 5 (left). Exchange fraction,  $F_{\Sigma}$ , plotted against the exchange time  $t_E$  (in minutes, logarithmic scale) in (i, ii)  $AgI$  ( $0.0425$  M and  $0.0450$  M) +  $0.05$  M  $KI(^{131}I)$  and (iii, iv)  $PbI_2$  ( $0.0050$  M and  $0.0075$  M) +  $0.05$  M  $KI(^{131}I)$  systems aged for  $t_A = 10$  minutes at  $293$  K.

Figure 6 (right). Exchange fractions  $F_{\Sigma}$  [eq. 1],  $F_{(\Sigma)R}$  [eq. 2] and  $F_{\sigma}$  [eq. 3] plotted against exchange time  $t_E$  (in minutes, logarithmic scale) in

$[F_{\Sigma}]$   $PbI_2$  ( $f_{Pb} = 0.15; 0.015$  m/l) +  $AgI$  ( $f_{Ag} = 0.85; 0.0425$  m/l) +  $0.05$  M  $KI(^{131}I)$ ;

$[F_{(\Sigma)R}]$   $PbI_2$  ( $0.025$  m/l) +  $0.05$  M  $KI(^{131}I)$  and  $AgI$  ( $0.05$  m/l) +  $0.05$  M  $KI(^{131}I)$ ;

$[F_{\sigma}]$   $AgI$  ( $0.0425$  m/l) +  $0.05$  M  $KI(^{131}I)$  and  $PbI_2$  ( $0.015$  m/l) +  $0.05$  M  $KI(^{131}I)$  systems aged for  $t_A = 10$  minutes at  $293$  K.

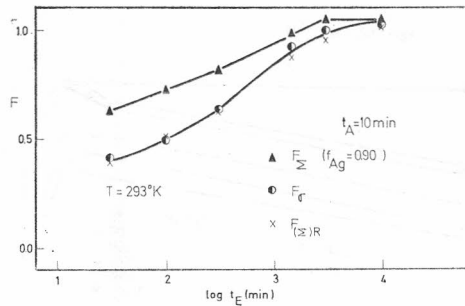


Figure 7. Exchange fractions  $F_{\Sigma}$  [eq. 1],  $F_{(\Sigma)R}$  [eq. 2] and  $F_{\sigma}$  [eq. 3] plotted against exchange time  $t_E$  (in minutes, logarithmic scale) in

$[F_{\Sigma}]$   $\text{PbI}_2$  ( $f_{\text{Pb}} = 0.10$ ; 0.01 m/l) +  $\text{AgI}$  ( $f_{\text{Ag}} = 0.90$ ; 0.045 m/l) + 0.05 M  $\text{KI}^{(131)\text{I}}$  system;  
 $[F_{(\Sigma)R}]$   $\text{PbI}_2$  (0.025 m/l) + 0.05 M  $\text{KI}^{(131)\text{I}}$  and  $\text{AgI}$  (0.050 m/l) + 0.05 M  $\text{KI}^{(131)\text{I}}$  system;  
 $[F_{\sigma}]$   $\text{AgI}$  (0.045 m/l) + 0.05 M  $\text{KI}^{(131)\text{I}}$  and  $\text{PbI}_2$  (0.01 m/l) + 0.05 M  $\text{KI}^{(131)\text{I}}$  systems aged for  $t_A = 10$  minutes at 293 K.

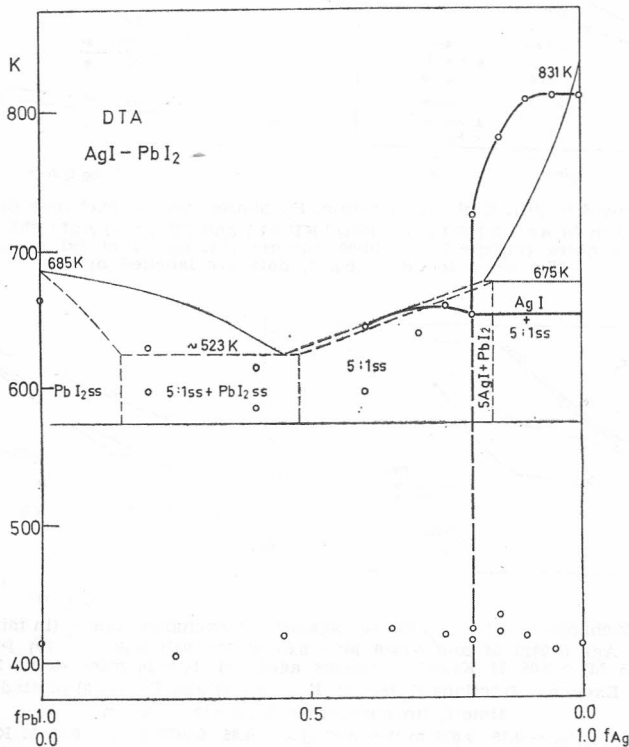
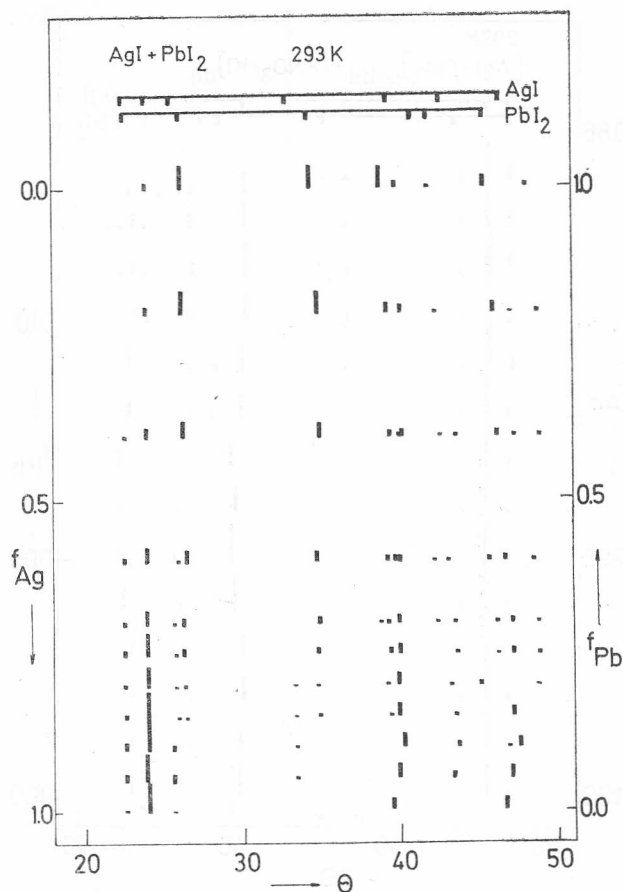


Figure 8. Phase diagram of the  $\text{PbI}_2 + \text{AgI}$  system. Ordinate; temperature of the system, abscissa; mole fraction of  $\text{PbI}_2$  or  $\text{AgI}$  in the initial mixture. Thin line; ref. 6.



Figures 9 and 10. Relative intensities of the most prominent diffraction lines of  $\text{PbI}_2$  and  $\text{AgI}$  (washed and dried samples; Figure 9 and precipitates in contact with original supernatant solution; Figure 10). Ordinate; mole fractions  $f$  of  $\text{AgI}$  ( $f_{\text{Ag}}$ ) and  $\text{PbI}_2$  ( $f_{\text{Pb}}$ ) and corresponding relative intensities represented by the length of mark, abscissa; diffraction angles.

aluminium cup was used. The heating rate was  $10 \text{ K/min}$ . The results are presented as the transition temperature *versus* molar ratio of  $\text{AgI}$  and  $\text{PbI}_2$  in analysed samples. See Figure 8.

#### X-Ray Diffraction Analysis

The structural properties of the  $\text{AgI} + \text{PbI}_2$  systems '*in statu nascendi*' prepared in various  $\text{AgI/PbI}_2$  molar ratios were examined by X-ray diffraction (RTG) using a Philips diffractometer with a scintillation counter and a single-channel pulse height analyser. The radiation was Ni-filtered  $\text{Cu K}\alpha$ . X-ray patterns were taken from the vacuum dried samples previously washed, and from the sample in contact with the original supernatant solution. Several independent experiments were run with each sample and it was found that the preferred orientation of the precipitate particles could be neglected. The relative intensities of the most prominent diffraction lines of  $\text{AgI}$  and  $\text{PbI}_2$  for various  $\text{AgI/PbI}_2$  molar ratios, are shown in Figures 9 and 10 for Bragg angles from  $2\theta = 20^\circ$  to  $2\theta = 50^\circ$ .

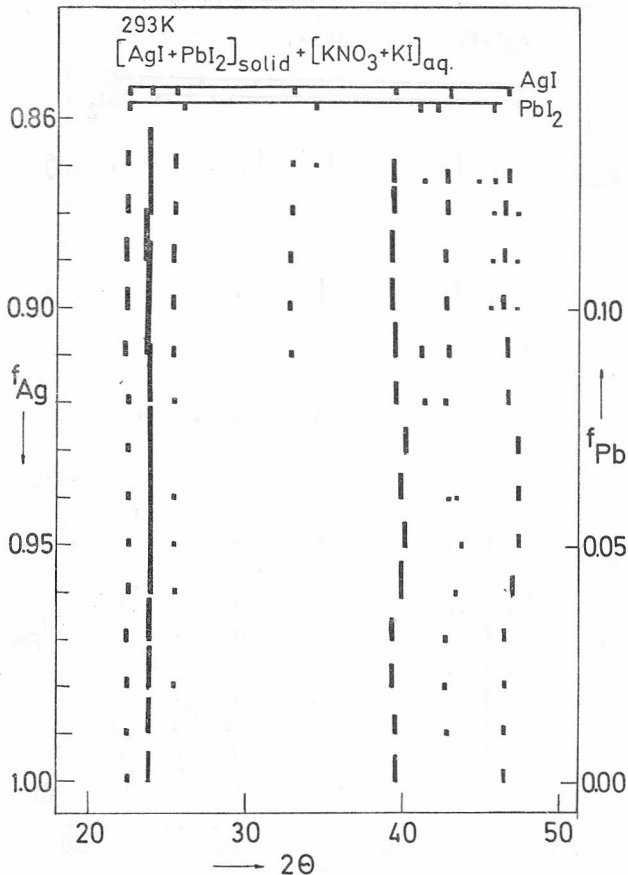


Figure 10.

## RESULTS AND DISCUSSION

The poorly soluble lead iodide is in contact with the well soluble potassium iodide in aqueous media. The iodide anion, common for both compounds was labelled by  $^{131}\text{I}$ . The total amount number of moles of iodide in the liquid phase is  $n_{\text{R}}^{\text{L}}$ , in the solid phase  $n_{\text{R}}^{\text{S}}$ , and the ratio is  $\alpha_{\text{R}} = n_{\text{R}}^{\text{S}}/n_{\text{R}}^{\text{L}}$ . In  $\text{PbI}_2 + \text{KI}$  systems in aqueous media the solubility of  $\text{PbI}_2$  is measurable, then  $n_{\Sigma}^{\text{L}} = n_{\text{KI}}^{\text{L}} + n_{\text{PbI}_2}^{\text{L}}$  and  $\alpha_{\Sigma} = n_{\Sigma}^{\text{S}}/n_{\Sigma}^{\text{L}} = n_{\text{PbI}_2}^{\text{S}}/(n_{\text{KI}}^{\text{L}} + n_{\text{PbI}_2}^{\text{L}})$ . Under conditions at which  $n_{\text{PbI}_2}^{\text{L}}$  is equal to zero,  $\text{PbI}_2$  will be present in the studied system in the form of precipitate. Then  $\alpha_{\Sigma}$  will be equal to  $\alpha_{\text{R}}$ . The  $\alpha_{\text{R}}$  values were calculated on the basis of the amounts of the precipitating components and assuming  $\text{PbI}_2$  to be insoluble. The real  $\alpha$  values were radiometrically determined as  $\alpha_{\Sigma} = (A_0 - A_{\infty})/A_{\infty}$ . If the determined  $\alpha_{\Sigma}$  is smaller than  $\alpha_{\text{R}}$ ,  $n_{\Sigma}^{\text{S}}$  is smaller than  $n_{\text{R}}^{\text{S}}$ . Then  $n_{\Sigma}^{\text{L}}$  must be greater than  $n_{\text{R}}^{\text{L}}$  and the solubility of  $\text{PbI}_2$  increases. The solubility of lead iodide is dependent on the presence of both iodide<sup>3</sup> and nonhalide<sup>4</sup> ions in the solution. Radiometric analysis of the  $\text{PbI}_2 + \text{KI}$  systems show (Figure 1) approximately equal solubility of  $\text{PbI}_2$

( $\alpha_{\Sigma} = 1.0$ ) in 0.01 M to 0.2 M KI, and according to literature data<sup>3</sup> at higher KI concentrations the solubility of the  $\text{PbI}_2$  increases ( $\alpha_{\Sigma} < 1$ ). An increase of the  $\text{PbI}_2$  solubility at KI concentrations lower than 0.01 M is a consequence of dilution. In the systems with 0.4 M  $\text{KNO}_3$  the solubility curve is shifted toward higher KI concentration. In the case of  $\text{PbI}_2 + \text{AgI} + \text{KI} + \text{KNO}_3$  in the system  $n_{\Sigma}^{\text{S}} = n_{\text{PbI}_2}^{\text{S}} + n_{\text{AgI}}^{\text{S}}$  and  $n_{\Sigma}^{\text{L}} = n_{\text{KI}}^{\text{L}} + n_{\text{PbI}_2}^{\text{L}} + n_{\text{AgI}}^{\text{L}}$  or  $\alpha_{\Sigma} = n_{\Sigma}^{\text{S}}/n_{\Sigma}^{\text{L}}$ . The meaning of  $\alpha_{\Sigma}$  is the same as before, except that the solubility of metal iodides is represented as a sum. The results of radiometric analyses (Table I) show that  $\alpha_{\Sigma}$  is independent of mole fractions  $f$  of both silver iodide ( $f_{\text{AgI}}$ ) and lead iodide ( $f_{\text{PbI}_2}$ ) at observed conditions. These radiometric results are in very good agreement with the above mentioned results and with the solubility data on silver iodide<sup>5</sup>. With respect to the metal halide solubilities, the heterogeneous exchange process at 0.05 M KI for mixed  $\text{PbI}_2 + \text{AgI}$  precipitates can be calculated on the basis of simple homogeneous distribution of the radioactivity; the fraction of exchange  $F = (A_0 - A_t)/(A_0 - A_{\infty})$  [eq. 1] where  $A_0$  represents the radioactivity of the liquid phase at time  $t$ , while  $A_{\infty}$  corresponds to the equilibrium radioactivity of the liquid phase and can be calculated as  $A_{\infty} = A_0/(1 + \alpha_{\Sigma})$ . In the systems with mixed precipitates the value  $F$  is represented by  $F_{\Sigma}$  without regard to the partial  $F$  values. The obtained results show (Figure 2) that the exchange fraction values are dependent on the mole fractions  $f_{\text{Pb}}$  and  $f_{\text{Ag}}$ . An increase of  $F_{\Sigma}$  values with  $t_{\text{E}}$  is in good agreement with the Ostwald's ripening process, well described in the case of  $(\text{AgI})_{\text{solid}} \leftrightarrow (\text{I}^-)_{\text{electrolyte solution}}$  systems<sup>1</sup>. However, the results for the systems with  $f_{\text{Ag}} = 0.85$  to  $0.95$ , show surprising increases in  $F$  values (Figures 2, 3, and 4), and the ageing effect ( $t_{\text{A}} = 10$  against  $t_{\text{A}} = 1000$  minutes aged systems) is together very strong<sup>1</sup>, indicating certain mutual phenomena in the systems under examination. Lower exchange fraction values for pure  $\text{PbI}_2$  than for pure  $\text{AgI}$  under equal conditions are a consequence of a markedly faster Ostwald ripening process in the systems with  $\text{PbI}_2$ . The ripening process of  $\text{AgI}$  particles is noticeably influenced by the presence of lead iodide. Taking into account the separate fractions of exchange for silver iodide,  $f_{\text{Ag}} \cdot F_{\text{Ag}}$ , and lead iodide,  $f_{\text{Pb}} \cdot F_{\text{Pb}}$ , where  $f$  represents the corresponding mole fraction, while  $F$  is the exchange value obtained at  $f = 1$ , the total average exchange fraction if  $F_{(\Sigma)\text{R}} = f_{\text{Ag}} \cdot F_{\text{Ag}} + f_{\text{Pb}} \cdot F_{\text{Pb}}$  [eq. 2]. Calculated  $F_{(\Sigma)\text{R}}$  values are approximately the same as the measured  $F_{\Sigma}$  values for the silver iodide system ( $f_{\text{Ag}} = 1.0$ , Figure 3). In this way the exchange fraction values calculated by equations [1] and [2] are mainly of a numeric nature although by detailed analysis of the » $F_{\Sigma}$  vs.  $\log t_{\text{E}}$ « curves it can be concluded that certain phenomena are taking place. In order to try to solve the problem the  $(\text{AgI})_{\text{solid}} \leftrightarrow (\text{I}^-)_{\text{electrolyte solution}}$  systems with  $\alpha_{\text{R}} = 0.85$  and  $0.90$  and  $(\text{PbI}_2)_{\text{solid}} \leftrightarrow (\text{I}^-)_{\text{electrolyte soln.}}$  systems with  $\alpha_{\text{R}} = 0.10$  and  $0.15$  were analysed. The results obtained (Figure 5) are in agreement with those presented in Figure 3, and quantitative data were used in the calculations of the sums of partial exchange fraction data corresponding to the assumed systems with virtual mole fractions  $f'$ ;  $f_{\text{Pb}}' = 0.15$ ,  $f_{\text{Ag}}' = 0.85$  (Figure 6) and  $f_{\text{Pb}}' = 0.10$ ,  $f_{\text{Ag}}' = 0.90$  (Figure 7):  $F_{\sigma} = f_{\text{Pb}}' \cdot F_{\text{Pb}}' + f_{\text{Ag}}' \cdot F_{\text{Ag}}'$  [eq. 3]. In both cases (Figures 6 and 7)  $F_{\Sigma}$  values were markedly higher than both the very similar  $F_{(\Sigma)\text{R}}$  and  $F_{\sigma}$  values. The noncongruity between measured and calculated  $F$  values indicates that the precipitated  $\text{PbI}_2 + \text{AgI}$  in KI solution is not a simple physical mixture, although there are no  $\text{PbI}_2$ — $\text{AgI}$  interactions known at equal

experimental conditions. DTA data<sup>6</sup> obtained for dried heated and cooled samples indicate  $\text{PbI}_2$ — $\text{AgI}$  interactions, while for the heated *in statu nascendi* prepared systems, no formation of  $\text{PbI}_2$ — $\text{AgI}$  compounds could be observed (Figure 8).

The structural properties of the metal halides present in mixtures were determined by X-ray diffraction analysis (RTG). In Figure 9, the relative intensities of the most prominent diffraction lines of metal halides are shown. The results obtained for the systems at  $f_{\text{Ag}} = 0.85$  to  $f_{\text{Ag}} = 0.95$  indicate the shift of diffraction lines, and the RTG data of these systems are collected in Figure 10. The shift of the diffraction line near  $2\theta = 40^\circ$  lies between diffraction lines of  $\text{AgI}$  and  $\text{PbI}_2$ , indicating that present metal halides are possibly partially grown into one crystal plane. DTA and RTG data do not indicate the existence of intermolecular  $\text{PbI}_2$ — $\text{AgI}$  compounds. On the basis of radiometric analysis we can draw the conclusion that the observed systems are not simple mixtures. Because of a strong influence of the ageing on the properties of the system it would be appear reasonable to conclude that the properties of  $\text{AgI} + \text{PbI}_2$  precipitates are influenced by the colloid interactions throughout the *in statu nascendi* precipitation, *i. e.* by the embryonation, nucleation and aggregation processes.

#### REFERENCES

1. R. Despotović, *Disc. Faraday Soc.* **42** (1966) 208; R. Despotović in A. L. Smith (Ed.), *»Particle Growth in Suspensions«*, Academic Press, London — New York (1973) p. 121; R. Despotović and B. Subotić, *J. Inorg. Nucl. Chem.*, **38** (1976) 1317.
2. A. C. Wahl and N. A. Bonner in J. Wiley (Ed.), *»Radioactivity Applied to Chemistry«*, New York (1951).
3. H. S. van Klooster and P. A. Balon, *J. Amer. Chem. Soc.* **56** (1934) 591; L. Roger, *Compt. rend.* **206** (1938) 1181, **211** (1940) 388; E. A. Gyunner and N. D. Yakhind, *Krym. Pedagog. Inst. im Frunze, Simferopol, USSR, Ukr. Khim. Zh.* **36**, 2 (1970) 147.
4. R. N. Golovaty, *J. Applied Chem.* **13** (1940) 586; F. Ya. Kul'ba, V. E. Mironov, and G. N. Kolyushenkova, *Zh. Neorgan. Khim.* **9** (1964) 1638.
5. J. Kratochvil, B. Težak, and V. B. Vouk, *Croat. Chem. Acta* **26** (1954) 191.
6. E. E. Frank Germann and Ch. F. Metz, *J. Phys. Chem.* **35** (1931) 1949; *»Phase Diagrams for Ceramics, 1969, Supplement (Figures 2067—4149)«* Compiled by E. M. Levin, C. R. Rabbins, and H. F. McMurdie at the National Bureau of Standards, Ed. & Publ. American Ceramic Society, Inc. 1969.
7. H. E. Schwiete and G. Ziegler, *Ber. Deutsch. Keram. Gesel.* **35** (1968) 193.

#### SAŽETAK

#### Heterogena zamjena mješanih taloga. $[\text{AgI} + \text{PbI}_2]_{\text{čvrsto}}$ u otopini KI

R. Despotović, Z. Despotović, S. Popović, L. Prodanović i B. Tomaš

Istraživan je tok procesa heterogene zamjene mješanih taloga  $\text{PbI}_2 + \text{AgI}$  i jodidnih iona u otopini KI s pomoću radioaktivnog  $^{131}\text{I}$ . Istraživani sistemi priređeni su *in statu nascendi* na 293 K. Radiometrijski određena topljivost, podaci diferencijalne termičke analize i difraktometrijske analize uspoređeni su s radioanalitičkim rezultatima procesa heterogene zamjene. Rezultati pokazuju izrazitu međusobnu ovisnost prisutnih metalnih halogenida u toku procesa zamjene. Kvantitativna analiza radiometrijskih podataka upućuje na specifično djelovanje olovnog jodida na čestice srebrnog jodida u toku Ostwaldova zrijenja.